Tohoku J. Exp. Med., 2021, **254**, 221-231

Long Non-Coding RNA SOX2 Overlapping Transcript Aggravates H9c2 Cell Injury via the miR-215-5p/ZEB2 Axis and Promotes Ischemic Heart Failure in a Rat Model

Jiahong Tu,[1] Liping Ma,[1] Mingqing Zhang[1] and Jie Zhang[2]

[1]Department of Emergency, Beijing Jishuitan Hospital, Beijing, China
[2]Department of Anesthesiology, Dongzhimen Hospital Beijing University of Chinese Medicine, Beijing, China

Heart failure is a common cardiovascular disease, which has been regarded as one of the highest health care costs with high morbidity and mortality in the western countries. Long noncoding RNAs have been widely reported to regulate the initiation or progression of cardiovascular diseases. However, the specific role of SOX2 overlapping transcript (SOX2-OT) in ischemic heart failure remains uncharacterized. The present study aimed to explore the function and mechanism of SOX2-OT in ischemic heart failure. The starBase website was used to predict potential miRNAs or target mRNAs. Western blot assay was implemented to test collagen protein levels. Functional assays were conducted to evaluate the effects of SOX2-OT on H9c2 cell viability and apoptosis. RNA pull down and luciferase reporter assays were used to confirm the combination between miR-215-5p and SOX2-OT. We found out that SOX2-OT level was increased by oxygen glucose deprivation/reoxygenation treatment in H9c2 cells. Silencing of SOX2-OT ameliorated cell injury by promoting cell viability, inhibiting cell apoptosis and reducing productions of collagens. Mechanistically, miR-215-5p was confirmed to bind with SOX2-OT after prediction and screening. In addition, we discovered that miR-215-5p negatively regulated zinc finger E-box binding homeobox 2 (ZEB2) protein level by directly binding with ZEB2 3′ untranslated region. Finally, we verified that SOX2-OT aggravated cell injury by targeting ZEB2 in H9c2 cells**.** In conclusion, SOX2-OT aggravated heart failure *in vivo* and promoted H9c2 cell injury via the miR-215-5p/ZEB2 axis *in vitro*, implying a novel insight into heart failure treatment.

Keywords: H9c2 cell injury; ischemic heart failure; miR-215-5p; SOX2-OT; ZEB2
Tohoku J. Exp. Med., 2021 July, **254** (3), 221-231.

Introduction

Heart failure, a common cardiovascular disease, is characterized by cardiomyocyte injury and contributes to insufficient supply of blood for activities and metabolism of organs (Huynh 2016; Rossello et al. 2016). As a result, the heart becomes enlarged and loses function (Henry and Armstrong 2016). Heart failure has been regarded as one of the highest health care costs with high morbidity and mortality in the western countries (Boully and Hanon 2015). Medical and surgical reperfusion has been considered to be effective therapeutic strategies for ischemic heart disease treatment (Heusch and Gersh 2017). However, accumulating evidence indicated that ischemia-reperfusion injury was easily induced when the blood reflows to ischemic myocardium (Curran et al. 2019).

According to the encyclopedia of DNA elements project, at least 80% of the genome is transcribed into protein coding RNAs (1%-1.5%) and a much larger number of noncoding RNAs (ENCODE Project Consortium 2012) that are arbitrarily divided into short (< 200 nt) and long (lncRNAs, > 200 nt) RNAs (ENCODE Project Consortium 2004). Long noncoding RNAs have been widely reported to regulate the initiation or progression of cardiovascular diseases (Uchida and Dimmeler 2015; Huang 2018). For instance, metastasis associated lung adenocarcinoma transcript 1 modulated cardiac inflammation and dysfunction induced by sepsis through the miR-125b/p38 axis (Chen et al. 2018). HOX Transcript Antisense RNA facilitated inflammatory response by upregulating receptor for advanced gly-

Received February 26, 2021; revised and accepted May 3, 2021. Published online July 29, 2021; doi: 10.1620/tjem.254.221.
Correspondence: Jie Zhang, Dongzhimen Hospital Beijing University of Chinese Medicine, No. 5 Shipping Warehouse, Dongcheng District, Beijing 100700, China.
e-mail: doczj000@163.com

cation end-products after acute myocardium infarction (Lu et al. 2018). Recently, SOX2 overlapping transcript (SOX2-OT) was reported to act as an oncogene in various tumors (Wang et al. 2017; Wei et al. 2018; Tai et al. 2019). Furthermore, SOX2-OT was indicated to be significantly upregulated in patients with non-end-stage heart failure based on RNA profiling results (Greco et al. 2016).

MicroRNAs (miRNAs), a subgroup of short noncoding RNAs with approximately 22 nucleotides in size, are single stranded (Lu and Rothenberg 2018). Although miRNAs are unable to encode proteins, they can bind with the 3′ untranslated region of mRNAs to inhibit translation, thereby exert effects on diverse biological processes (Cai et al. 2009). As example, miR-21-5p modulated acute drug-induced cardiac injury by affecting inflammatory infiltration in rats (Gryshkova et al. 2018). In addition, miR-150 ameliorated ischemic injury by modulating cell death in mice (Tang et al. 2015). Importantly, miR-215-5p was confirmed to be associated with the progression of doxorubicin-induced cardiotoxicity *in vivo* (Ruggeri et al. 2018).

The current exploration was aimed to figure out the biological function and potential mechanism of SOX2-OT in oxygen glucose deprivation/reoxygenation-induced H9c2 cellular injury model. At first, we established ischemic cell model and rat model. Second, we evaluated the effects of SOX2-OT on ischemic heart failure *in vitro* and *in vivo*. At last, we further investigated the regulatory mechanism of SOX2-OT in *in vitro* model. We found out that SOX2-OT aggravated ischemic heart failure in rats and promoted H9c2 cell injury via the miR-215-5p/ZEB2 axis in H9c2 cells, implying a novel insight into heart failure treatment.

Materials and Methods

Animals

Sprague-Dawley rats weighing 250-320 g (Beijing Vital River Laboratory Animal Technology Co., Ltd., Beijing, China) were housed in a specific pathogen-free room at 24°C ± 2°C and humidity (55 ± 10%) and had free access to standard rat chow and water. The research protocol was approved by the Institutional Animal Care and Use Committee of Dongzhimen Hospital Beijing University of Chinese Medicine and conformed to the Guide for Use of Laboratory Animals.

Adeno associated virus (AAVs) and animal grouping

Empty AAV vector (serotype: AAV9) and AAV-sh-SOX2-OT were provided by GenePharma (Shanghai, China). Rats were randomly assigned to 4 different groups: sham group, ischemic heart failure group, ischemic heart failure + AAV-NC group and ischemic heart failure + AAV-sh-SOX2-OT group. AAVs (5×10^{12} genome containing particles) were injected into the heart of rats using a 30-gauge needle.

Establishment of the ischemic heart failure rat model

All experimental rats were anesthetized by intraperitoneal injection of 7% chloral hydrate. After left thoracotomy and pericardiotomy, left coronary artery was dissected above the first diagonal branch. The left circumflex arterial origin was immediately ligated with silk thread. Slipknot-induced occlusion lasted for 30 min, and then myocardium distal was observed darkened.

Hematoxylin and eosin staining

Cardiac tissues were taken from the central part of the left ventricle and was fixed in polyoxymethylene for 24 h, dehydrated in ethanol, permeabilized in PBST, embedded in paraffin. Next, paraffin sections (5 μm) were dewaxed by xylene for 10 min, and hydrated by gradient ethanol for 1 min followed by washing with water for 2 min. Subsequently, sections were stained with hematoxylin for 4 min and then stained with eosin for 2 min following dehydration using gradient ethanol. The myocardial tissue morphology changes were observed under the microscope.

Enzyme-linked Immunosorbent Assay (ELISA)

Four weeks after the operation, 10 mL fasting venous blood of rats were taken from the right carotid artery under the aseptic condition. The serum level of B-type natriuretic peptide (BNP) was measured using a BNP ELISA Kit (ab108815; Abcam, Cambridge, UK) and that of endothelin 1 was measured using an endothelin 1 ELISA Kit (ab133030; Abcam) based on the manufacturer's instructions.

Cells and cell treatment

H9c2 cells (Chinese Academy of Sciences, Shanghai, China) were cultured in high-glucose Dulbecco's Modified Eagle Medium (HyClone, Beijing, China) containing 10% fetal bovine serum (FBS; Thermo Fisher Scientific, Waltham, MA, USA) and 1% Penicillin/Streptomycin (100 U/ml:100 mg/ml) (Thermo Fisher Scientific). H9c2 cells were incubated at 37°C in a humidified atmosphere containing 5% CO_2. For oxygen glucose deprivation treatment, H9c2 cells was maintained at 37°C for 4 h in glucose-free Dulbecco's Modified Eagle Medium (Thermo Fisher Scientific) with 1% O_2 and 5% CO_2 to imitate ischemic injury *in vitro*. H9c2 cells were then cultivated at 37°C in normal culture medium under normoxic conditions (95% air, 5% CO_2) for 24 h. H9c2 cells the control group were treated identically but without oxygen glucose deprivation/reoxygenation.

Cell transfection

The SOX2-OT short hairpin RNA (shRNA) with negative control (sh-NC) was used to knocked down SOX2-OT. MiR-215-5p mimics with negative control (NC mimics) were used to overexpress miR-215-5p. The full length of ZEB2 was cloned into pcDNA3.1 vector to overexpress ZEB2 with empty pcDNA3.1 as control. The above-mentioned vectors (GenePharma, Shanghai, China) were transfected into H9c2 cells using Lipofectamine 2000 (Thermo

Fisher Scientific) 48 h before oxygen glucose deprivation reoxygenation.

Cell counting kit-8 (CCK-8) assay

The cell counting kit-8 (CCK-8; FUJIFILM Wako Chemicals, Tokyo, Japan) was used to measure cell viability. The transfected cells (5×10^4 cells/well) were grown in 96-well plate. After 48 h for cultivation, the supernatant fluid was removed. Then, cells were incubated with a medium containing 10% CCK-8 reagent for 2 h at 37°C. At last, the absorbance was measured by an AMR-100 automatic enzyme analyzer (Allsheng, Hangzhou, China) at 450 nm.

Flow cytometry assay

Cell apoptosis was evaluated by FITC Annexin V Apoptosis Detection Kit (BD Pharmingen™, Franklin Lakes, NJ, USA). Briefly, H9c2 cells were resuspended in a 1X Binding Buffer (5×10^5 cells/mL) after being washed with cold phosphate buffer saline (Sigma-Aldrich Co., St. Louis, MO, USA). Then, total 100 μL of cell solution (5×10^4 cells) was moved into a 5 mL culture tube. After addition of 5 μL of fluorescein isothiocyanate Annexin V and 5 μL of propidium iodide, H9c2 cells were gently vortexed and cultured in the dark for 15 min at room temperature. Subsequently, total 400 μL of 1X Binding Buffer was added. At last, apoptosis of H9c2 cells were analyzed via flow cytometry. The apoptotic cells were calculated by FlowJo software.

Determination of mitochondrial function

The ATP levels in the H9c2 cells were measured with an ATP Assay Kit (Jiancheng, Nanjing, China) following the manufacturer's instruction. Mitochondria were isolated from the H9c2 cells using a Tissue/Cell Mitochondria Isolation Kit (Beyotime Inc., Nantong, Jiangsu, China). Activities of mitochondrial complex I, complex II and complex IV were detected using corresponding assay kits (Jiancheng) based on the manufacturer's guidelines. The relative enzymatic activities of mitochondrial complexes are expressed as the difference in the absorbance at the corresponding wavelength over a 3-min reaction.

Intracellular reactive oxygen species detection

Cells were preloaded with 10 μM of 2, 7-dichlorofluorescin diacetate (DCFH-DA; Beyotime) for 20 min at 37°C. Afterward, the cells were washed using a culture medium without serum. A fluorescence microplate reader with an excitation wavelength of 488 nm and an emission wavelength of 525 nm was used to determine fluorescence intensity.

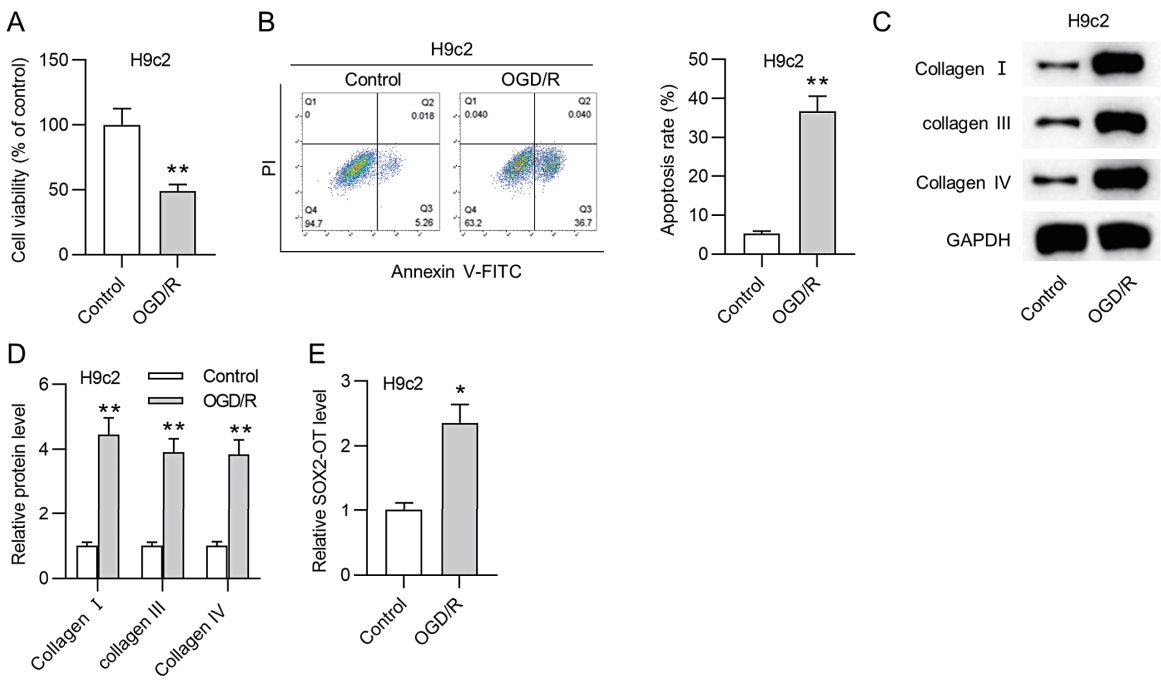

Fig. 1. SOX2-OT level was increased by oxygen glucose deprivation/reoxygenation treatment in H9c2 cells.
(A) Cell viability was detected by CCK-8 assay in H9c2 cells after oxygen glucose deprivation for 4 h and reoxygenation for 24 h. (B) Cell apoptosis was examined by flow cytometry in H9c2 cells after oxygen glucose deprivation for 4 h and reoxygenation for 24 h. (C-D) The protein levels of collagens were determined by western blot in H9c2 cells after oxygen glucose deprivation for 4 h and reoxygenation for 24 h. (E) SOX2-OT level was tested by RT-qPCR in H9c2 cells after oxygen glucose deprivation for 4 h and reoxygenation for 24 h. $^*P < 0.05$, $^{**}P < 0.01$. SOX2-OT, SOX2 overlapping transcript; OGD/R, oxygen glucose deprivation/reoxygenation; CCK-8, cell counting kit-8; RT-qPCR, reverse-transcription quantitative polymerase chain reaction.

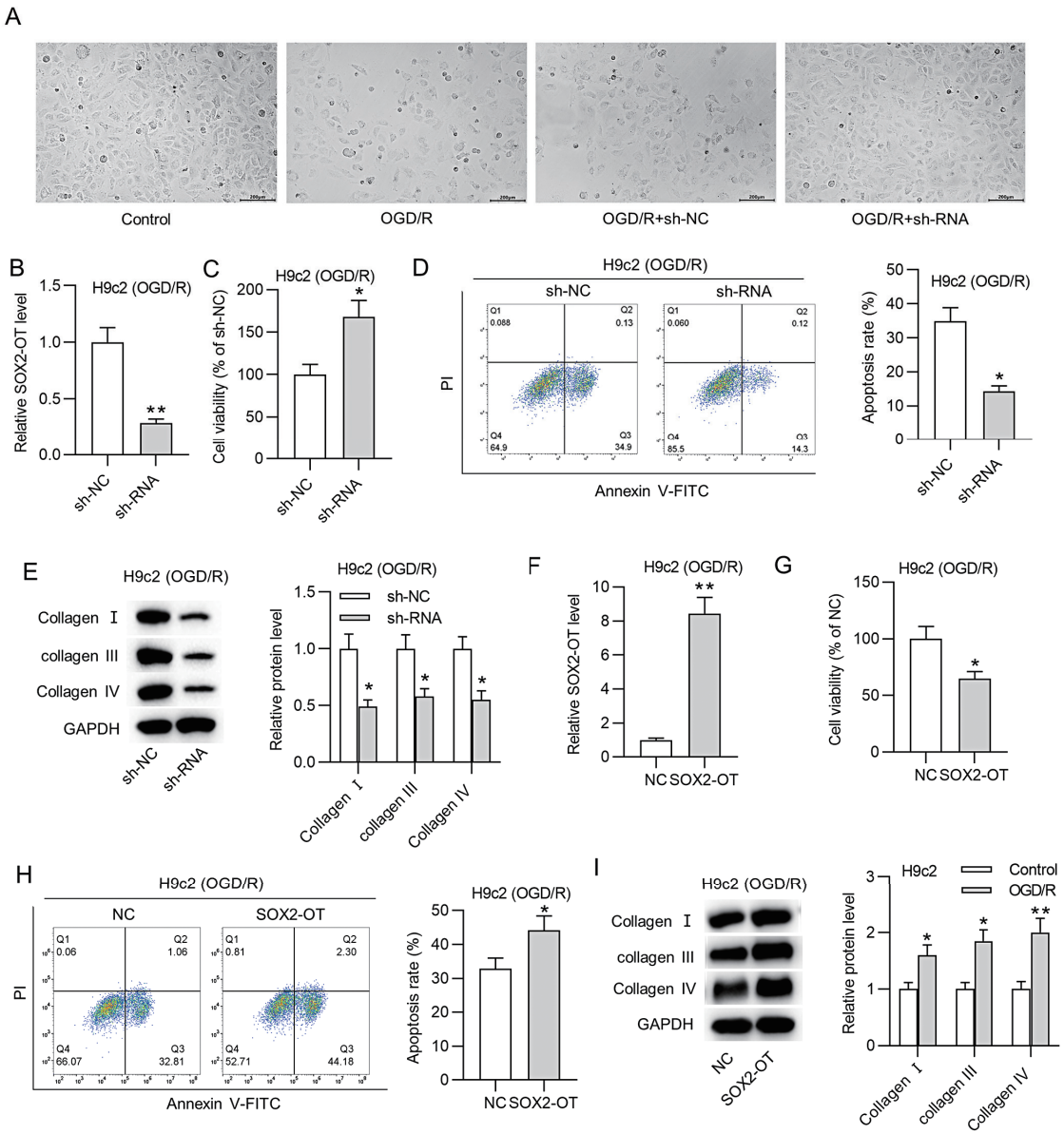

Fig. 2. Silencing of SOX2-OT ameliorated H9c2 cell injury.
(A) Images of H9c2 cells in different groups. (B) The knockdown efficacy of SOX2-OT sh-RNA in H9c2 cells was evaluated by RT-qPCR. (C) The effect of SOX2-OT sh-RNA on cell viability. (D) The effect of SOX2-OT sh-RNA on cell apoptosis. (E) The effect of SOX2-OT sh-RNA on collagen levels. (F) The overexpression efficacy of SOX2-OT in H9c2 cells was evaluated by RT-qPCR. (G-H) The effect of pcDNA3.1 vector containing SOX2-OT on cell viability and apoptosis. (I) The effect of SOX2-OT overexpression on collagen levels. H9c2 cells were transfected with sh-NC or SOX2-OT sh-RNA for 48 h followed by oxygen glucose deprivation for 4 h and reoxygenation for 24 h. $^{*}P < 0.05$, $^{**}P < 0.01$. SOX2-OT, SOX2 overlapping transcript; sh-RNA, short hairpin RNA; OGD/R, oxygen glucose deprivation/reoxygenation; RT-qPCR, reverse-transcription quantitative polymerase chain reaction.

Reverse-transcription quantitative polymerase chain reaction (RT-qPCR)

The extraction of total RNA from cardiac tissues or H9c2 cells was performed as described previously (Chen et al. 2018). The total RNA was reverse transcribed into cDNA using a Quantscript RT Kit (Tiangen-Biotech, Beijing, China). The iQ SYBR Green Supermix (Bio-Rad Laboratories, Hercules, CA, USA) was used for RNA analysis. The TanMan® microRNA Assay Kit (Thermo Fisher Scientific) was used for miRNA analysis. The relative level of RNAs were analyzed using the $2^{-\Delta\Delta Ct}$ method normalized to glyceraldehyde-3-phosphate dehydrogenase (for SOX2-OT and mRNA quantification) or U6 (for miRNA quantification).

Western blot

Western blot analysis was performed as previously described (Lu et al. 2018). In brief, protein was extracted

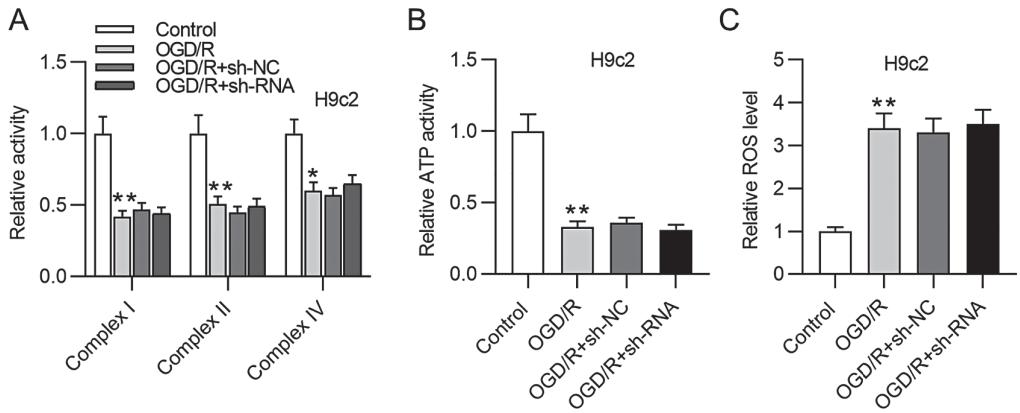

Fig. 3. Silencing of SOX2-OT had no effects on mitochondrial dysfunction.
(A) Relative activity of mitochondrial complex I, II and IV in H9c2 cells. (B) Relative ATP activity in H9c2 cells. (C) Relative ROS levels in H9c2 cells. H9c2 cells were transfected with sh-NC or SOX2-OT sh-RNA for 48 h followed by oxygen glucose deprivation for 4 h and reoxygenation for 24 h. $^{*}P < 0.05$, $^{**}P < 0.01$. SOX2-OT, SOX2 overlapping transcript; ATP, adenosine triphosphate; ROS, reactive oxygen species.

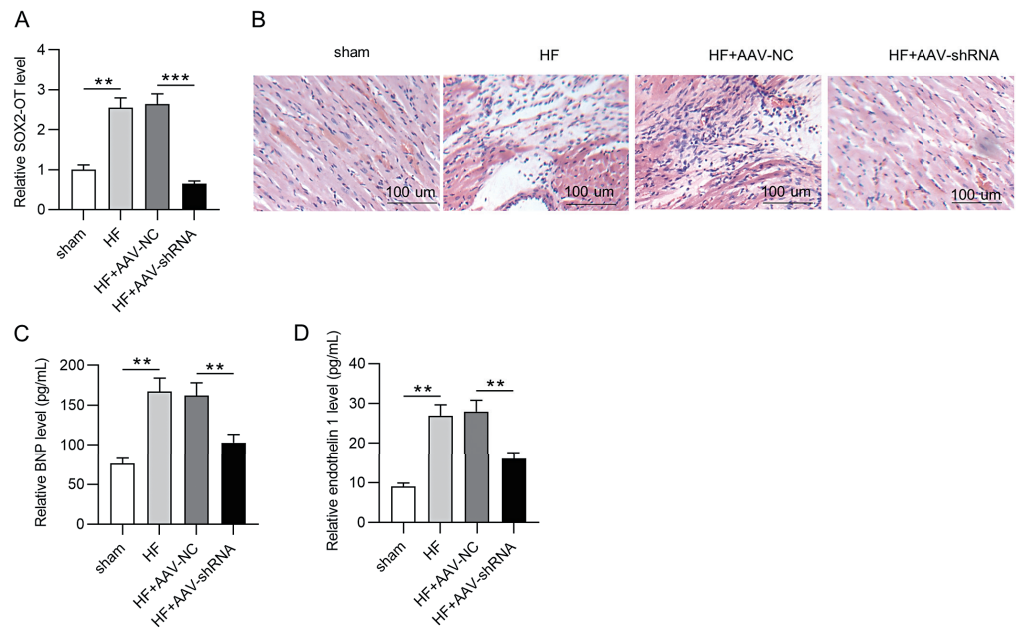

Fig. 4. SOX2-OT downregulation alleviated heart failure in rats.
(A) Relative SOX2-OT expression in cardiac tissues of rats in sham group, HF group, HF + AAV-NC group, and HF + AAV-SOX2-OT group. (B) Relative images of hematoxylin and eosin staining of cardiac tissues. (C) Relative BNP levels in serum of rats in sham group, HF group, HF + AAV-NC group, and HF + AAV-SOX2-OT group. (D) Relative endothelin 1 levels in serum of rats in sham group, HF group, HF + AAV-NC group, and HF + AAV-SOX2-OT group. $^{*}P < 0.05$, $^{**}P < 0.01$. SOX2-OT, SOX2 overlapping transcript; HF, heart failure; AAV, adeno-associated virus; NC, negative control; BNP, brain natriuretic peptide.

from H9c2 cells and subjected to sodium dodecyl sulfate polyacrylamide gel electrophoresis. Then, proteins were moved onto polyvinylidene difluoride membrane, which was then coated with defatted milk and blotted. Hereafter, the membranes were incubated with the primary antibodies including Collagen I antibody (ab270993; Abcam), Collagen II antibody (ab188570; Abcam) Collagen IV antibody (ab236640; Abcam), ZEB2 antibody (ab191364; Abcam) and GAPDH antibody (ab9484; Abcam) at 4°C overnight. A goat anti-mouse peroxidase-conjugated secondary antibody was added for incubation for another 4 hours at room temperature. The immunoreactive bands were visualized by enhanced chemiluminescence (SuperSignal West Femto Kit; Thermo Fisher Scientific) and quantified using Quantity One software (Alpha Innotech, San Leandro, CA, USA). GAPDH functioned as an internal control.

Table 1. Potential miRNAs containing the binding site on SOX2-OT.

Name	merClass	Sequence
miR-6088	8mer	gcGGGGGGGCG---AAGUAGAGa
miR-143-3p	8mer	cucgaugucacgaAGUAGAGu
miR-4770	8mer	ucGA-UGUCACAGUAGAGu
miR-452-5p	7mer-m8	agUCAAAGGAGACG-UUUGUCAa
miR-4676-3p	7mer-m8	uucucggucaccacUUUGUCAc
miR-892c-3p	7mer-m8	aggugagucuuuccUUUGUCAc
miR-192-5p	7mer-m8	ccGACAGUUAAGUAUCCAGUc
miR-215-5p	7mer-m8	caGACAGUUAAGUAUCCAGUa
miR-552-5p	8mer	ggUUGUCCGUUU---UCCAAUUUg
miR-186-5p	7mer-m8	ucGGGUUUUCCUCUUAAGAAAc
miR-654-3p	8mer	uuccacuaccaGUCGUCUGUAu
miR-3200-5p	8mer	uggAACACGCGGAAGAGUCUAa
miR-369-3p	7mer-m8	uuucuagUUGGUACAUAAUAa
miR-374a-5p	7mer-m8	gugAAUAGUCCAACAUAAUAUu
miR-374b-5p	7mer-m8	gugAAUCGUCCAACAUAAUAUa
miR-580-3p	7mer-m8	ggaUUACUAAGUAGUAAGAGUu
miR-676-3p	8mer	uugaguugUUGGAAUCCUGUc
miR-2355-3p	7mer-m8	uagaggUUUGUCGUUCCUGUUa
miR-409-3p	7mer-m8	uccccaagugGCUC-GUUGUAAg
miR-2681-5p	7mer-m8	ucagaggaccucCACCAUUUUg
miR-7151-5p	7mer-m8	cgguuaUGUCCGUCUCUACCUAg
miR-942-5p	8mer	guguACCGGUUUUGUCUCUUCu

Luciferase reporter assay

Luciferase reporter assay was used to evaluate the combination between miR-215-5p and SOX2-OT (or ZEB2 3′ untranslated region). In brief, firefly luciferase reporter vectors containing wild-type or mutated SOX2-OT (or ZEB2 3′ untranslated region) were purchased from GeneChem (Shanghai, China). The H9c2 cells were co-transfected with vectors containing wild-type or mutated SOX2-OT (or ZEB2 3′ untranslated region) and miR-215-5p mimics (or NC mimics) using Lipofectamine 2000 (Invitrogen). At last, the luciferase activities were evaluated by dual-luciferase reporter assay system (Promega, Madison, WI, USA).

RNA pull-down assay

Pull-down assay was used to evaluate the binding ability between SOX2-OT and potential miRNAs. First, the full-length of SOX2-OT was biotin-labeled and transcribed into H9c2 cells with the Biotin RNA Labeling Mix (Roche Diagnostics, Mannheim, Germany). After incubation for 48 h, H9c2 cells were lysed. Then, the cell lysates were mixed with biotin-labeled RNAs and cultivated with Streptavidin Dynabeads (Dyna beads M-280 Streptavidin, #11205D; Thermo Fisher Scientific). Finally, the RNAs pulled down by bio-SOX2-OT were purified and examined by RT-qPCR.

Statistical analysis

The data were presented as the mean ± standard deviation. Statistical analysis was performed using the SPSS software (Chicago, IL, USA). Comparisons between 2 groups (or more than 2 groups) were performed using Student's t tests or one-way analysis of variance followed by Tukey's *post hoc* analysis. Values of $P < 0.05$ were considered statistically significant.

Results

SOX2-OT level was increased by oxygen glucose deprivation/reoxygenation treatment in H9c2 cells

According to Fig. 1A, results of CCK-8 assay demonstrated that cell viability was decreased by oxygen glucose deprivation/reoxygenation treatment. Inversely, cell apoptosis was promoted by oxygen glucose deprivation/reoxygenation treatment (Fig. 1B). In addition, the collagen levels (collagen I, collagen III and collagen IV) were increased by oxygen glucose deprivation/reoxygenation treatment (Fig. 1C, D). All the data suggested that ischemic model was successfully established. Then, we detected SOX2-OT level in H9c2 cells. The result of RT-qPCR revealed that SOX2-OT level in oxygen glucose deprivation/reoxygenation group is higher than that in control group (Fig. 1E).

Silencing of SOX2-OT ameliorated H9c2 cell injury

We then explored the biological function of SOX2-OT in oxygen glucose deprivation/reoxygenation-treated H9c2 cells. Fig. 2A revealed that cell size was not significantly affected by oxygen glucose deprivation/reoxygenation, and

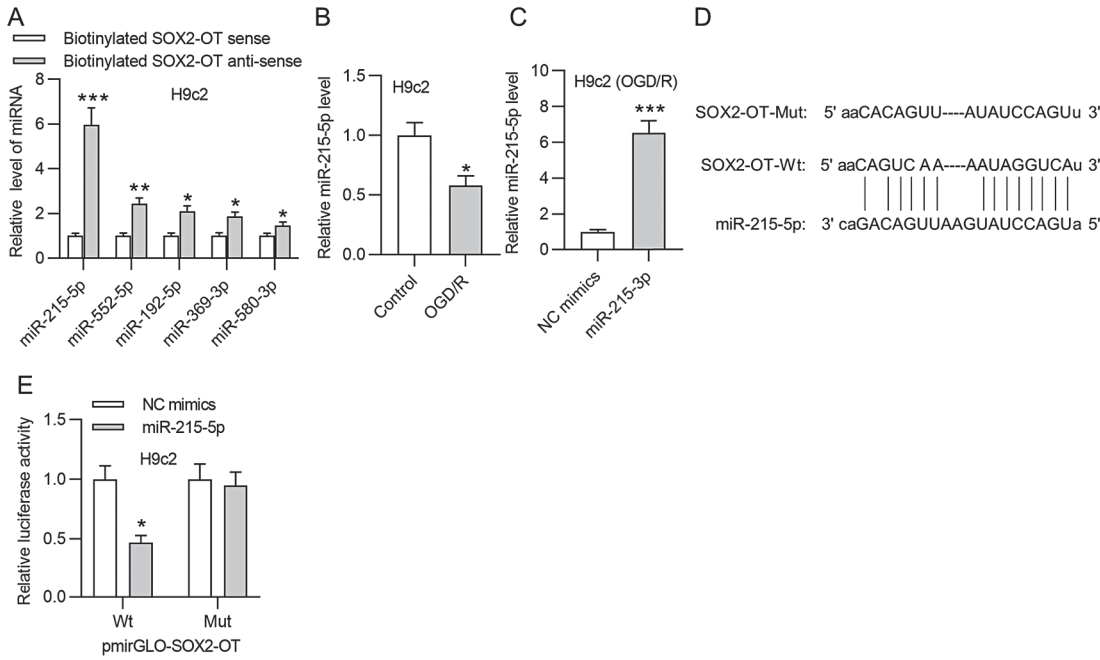

Fig. 5. SOX2-OT worked as a sponge for miR-215-5p.
(A) RNA pull down assay was used to assess the combination between SOX2-OT and potential miRNAs. (B) The miR-215-5p level in H9c2 cells after oxygen glucose deprivation for 4 h and reoxygenation for 24 h. (C) Overexpression efficacy of miR-215-5p in H9c2 cells transfected with miR-215-5p mimics for 48 h followed by oxygen glucose deprivation for 4 h and reoxygenation for 24 h were determined by RT-qPCR. (D) The binding sequences of miR-215-5p and SOX2-OT were predicted by starBase. (E) The luciferase reporter assay was used to evaluate the combination between miR-215-5p and SOX2-OT after transfection for 48 h. $^{*}P < 0.05$, $^{**}P < 0.01$, $^{***}P < 0.001$. SOX2-OT, SOX2 overlapping transcript; OGD/R, oxygen glucose deprivation/reoxygenation; RT-qPCR, reverse-transcription quantitative polymerase chain reaction.

downregulation of SOX2-OT had no significant effects on H9c2 cell size. At first, SOX2-OT level was effectively knocked down by transfection of SOX2-OT sh-RNA (Fig. 2B). Then, cell viability was promoted by SOX2-OT knockdown in oxygen glucose deprivation/reoxygenation-treated H9c2 cells (Fig. 2C). On the contrary, cell apoptosis was remarkedly inhibited by silencing of SOX2-OT in oxygen glucose deprivation/reoxygenation-treated H9c2 cells (Fig. 2D). Transfection of SOX2-OT sh-RNA lowered collagen levels including collagen I, collagen III and collagen IV in oxygen glucose deprivation/reoxygenation-treated H9c2 cells (Fig. 2E). Moreover, overexpression of SOX2-OT aggravates oxygen glucose deprivation/reoxygenation injury to H9c2 cells by decreasing cell viability, promoting apoptosis and increasing collagen protein levels (Fig. 2F-I).

Silencing of SOX2-OT had no effects on mitochondrial dysfunction

Relative mitochondrial complex I, complex II, complex IV activity was inhibited by oxygen glucose deprivation/reoxygenation, while silencing of SOX2-OT had no significant effects on mitochondrial complex I, complex II, complex IV activity (Fig. 3A). Similarly, ATP activity was suppressed by oxygen glucose deprivation/reoxygenation and was not significantly affected by silencing of SOX2-OT (Fig. 3B). Reactive oxygen species productions were higher in H9c2 cells after ischemic/reperfusion injury, and SOX2-OT downregulation had no significant effects on reactive oxygen species levels (Fig. 3C).

SOX2-OT downregulation alleviated heart failure in rats

SOX2-OT expression was higher in cardiac tissues of rats with heart failure than sham rats, and injection of AAV-sh-SOX2-OT decreased SOX2-OT expression (Fig. 4A). The results of hematoxylin and eosin staining assay showed that the myocardial fiber structure was clear and orderly arranged in the sham rats. Silencing of SOX2-OT attenuated myocardial structure disorders of muscle fibers and infiltration of inflammatory cells in cardiac tissues of model rats (Fig. 4B). Fig. 4C and D revealed that relative BNP and endothelin 1 levels were higher in model group than sham group, and SOX2-OT downregulation reduced BNP and endothelin 1 levels.

SOX2-OT worked as a sponge for miR-215-5p

Long noncoding RNA can act as a molecular sponge for miRNA to release the downstream target mRNA (Zhou et al. 2018; Zhang et al. 2020; Zou et al. 2020). We anticipated that SOX2-OT regulated H9c2 cell injury by this pattern. The bioinformatics tool (starBase: http://starbase.sysu.edu.cn/) was utilized to explore the potential miRNAs

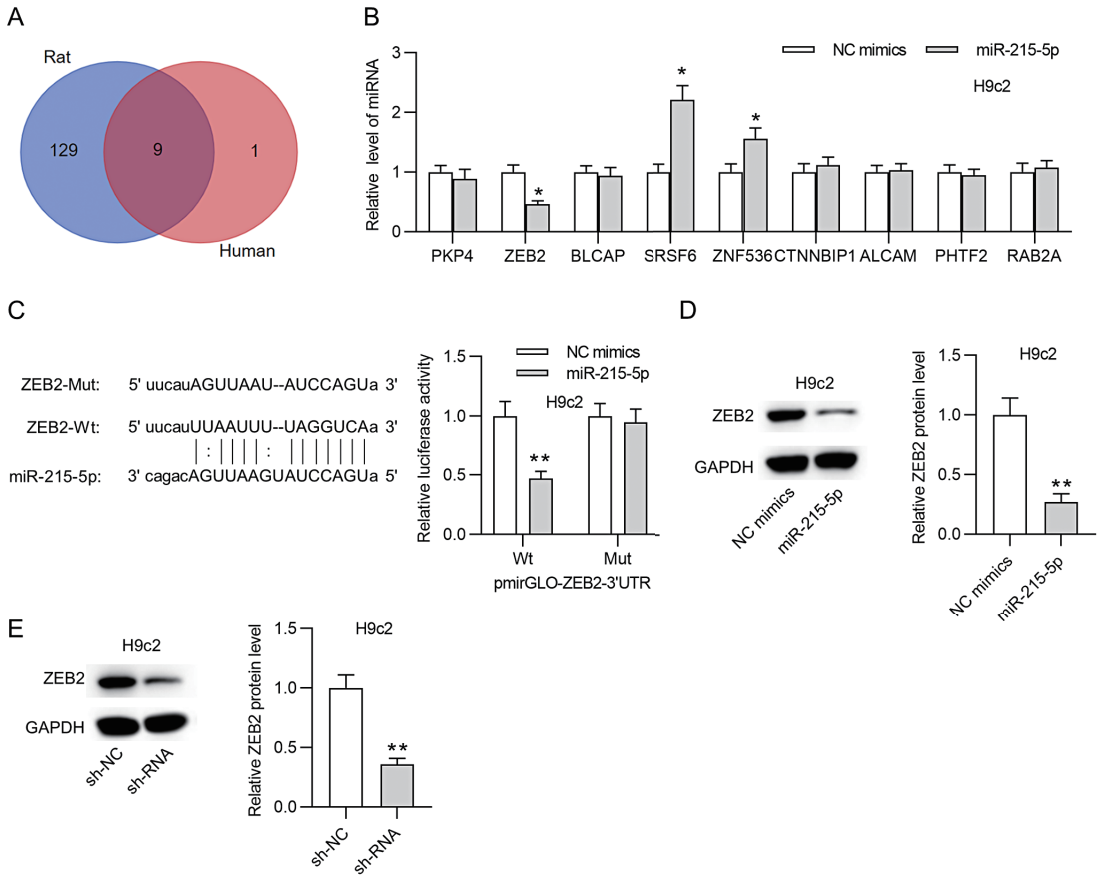

Fig. 6. MiR-215-5p directly targeted and negatively regulated ZEB2.
(A) The Venn diagram showed the potential target mRNAs of miR-215-5p. (B) The mRNA levels of PKP4, ZEB2, BLCAP, SRSF6, ZNF536, LRRFIP1, ADGRG6, PHFT2, RAB2A and CTNNBIP1 after transfection for 48 h were measured by RT-qPCR. (C) The binding site of miR-215-5p on ZEB2 3′ untranslated region was predicted by starBase, and luciferase reporter assay was utilized to validate the combination between miR-215-5p and ZEB2 3′ untranslated region after transfection for 48 h. (D-E) The protein level of ZEB2 in H9c2 cells after transfection of SOX2-OT shRNA and miR-215-5p mimics for 48 h was examined by western blot. $^{*}P < 0.05$, $^{**}P < 0.01$. SOX2-OT, SOX2 overlapping transcript; OGD/R, oxygen glucose deprivation/reoxygenation; ZEB2, zinc finger E-box binding homeobox 2; OGD/R, oxygen glucose deprivation/reoxygenation; RT-qPCR, reverse-transcription quantitative polymerase chain reaction.

that contain the binding site on SOX2-OT. According to Table 1, total 22 miRNAs harboring binding site on SOX2-OT were predicted. According to RNA pull down assay, only five miRNAs were significantly enriched in bio-SOX2-OT sense group, and miR-215-5p displayed the highest enrichment (Fig. 5A). Additionally, miR-215-5p level was reduced by oxygen glucose deprivation reoxygenation treatment (Fig. 5B). Then, we overexpressed miR-215-5p level by transfecting miR-215-5p mimics into H9c2 cells (Fig. 5C). The binding site between SOX2-OT and miR-215-3p was predicted by starBase (Fig. 5D). Finally, luciferase reporter assay revealed that miR-215-5p mimics lessened luciferase activity of wild type pmirGLO-SOX2-OT plasmid, and no alteration was observed in luciferase activity of mutated pmirGLO-SOX2-OT plasmid (Fig. 5E).

MiR-215-5p directly targeted and negatively regulated ZEB2

Hereafter, we aimed to figure out the target mRNAs of miR-215-5p. As shown in Venn diagram, total 9 mRNAs were screened out (Fig. 6A). Subsequently, we examined the expression of these mRNAs in H9c2 cells. Based on the results of RT-qPCR, we discovered that ZEB2 displayed low expression in response to miR-215-3p overexpression (Fig. 6B). Moreover, the luciferase activity of pmirGLO containing wild type ZEB2 3′ untranslated region was significantly lessened by miR-215-5p overexpression while luciferase activity of that containing mutated ZEB2 3′ untranslated region displayed no significant difference (Fig. 6C). Either miR-215-5p overexpression or SOX2-OT knockdown reduced ZEB2 protein levels in H9c2 cells (Fig. 6D, E).

SOX2-OT aggravated cell injury by ZEB2

To validate whether SOX2-OT promotes H9c2 cell injury by regulating ZEB2, rescue assays were conducted. To begin with, western blot assays showed that ZEB2 protein level was effectively increased by transfection of

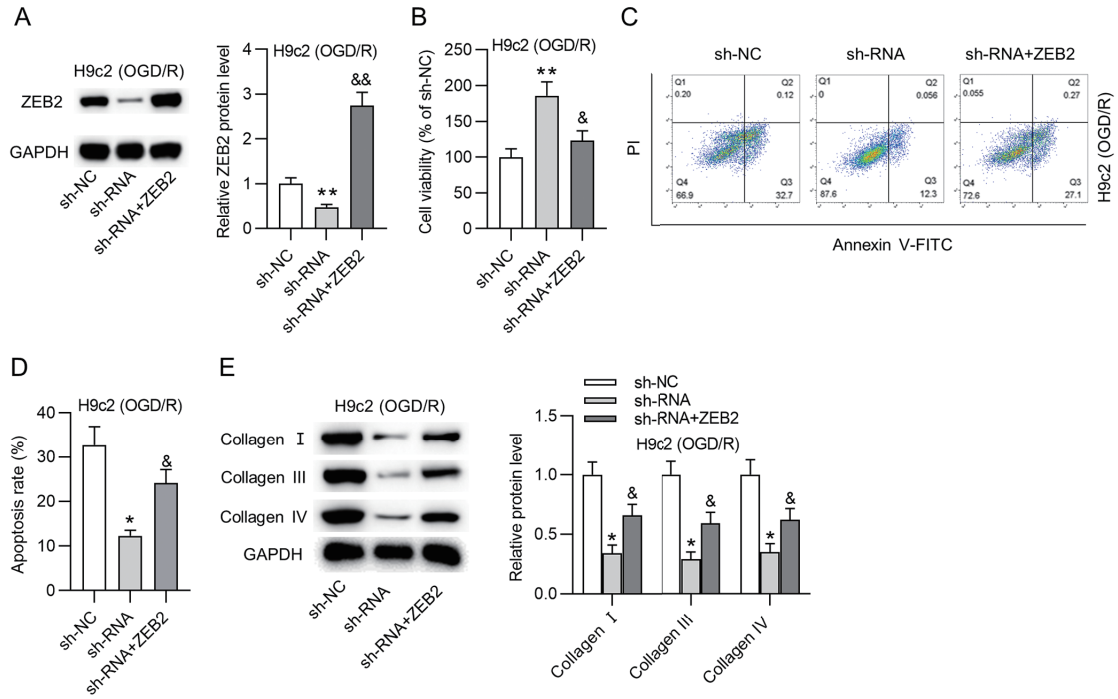

Fig. 7. SOX2-OT aggravated cell injury by ZEB2.
(A) The overexpression efficacy of ZEB2 was assessed by western blot. (B) The effect of SOX2-OT sh-RNA and pcDNA3.1/ZEB2 on cell viability. (C-D) The effect of SOX2-OT sh-RNA and pcDNA3.1/ZEB2 on cell apoptosis. (E) The effect of SOX2-OT sh-RNA and pcDNA3.1/ZEB2 on collagen levels. H9c2 cells were treated with OGD/R for 24 h and/or transfected with indicated plasmids for 48 h. $^{*}P < 0.05$, $^{**}P < 0.01$ compared with sh-NC group. $^{\&}P < 0.05$, $^{\&\&}P < 0.01$ compared with sh-RNA group. H9c2 cells were transfected with sh-NC, SOX2-OT sh-RNA or cotransfection of SOX2-OT sh-RNA + ZEB2 for 48 h followed by oxygen glucose deprivation for 4 h and reoxygenation for 24 h. SOX2-OT, SOX2 overlapping transcript; ZEB2, zinc finger E-box binding homeobox 2; sh-RNA, short hairpin RNA.

pcDNA3.1/ZEB2 (Fig. 7A). Furthermore, overexpression of ZEB2 offset the promotive effect of SOX2-OT sh-RNA on cell viability (Fig. 7B). Overexpression of ZEB2 neutralized the suppressive impact of SOX2-OT silencing on cell apoptosis (Fig. 7C, D). In addition, SOX2-OT sh-RNA mediated the reduction of collagen accumulation was counteracted by ZEB2 overexpression (Fig. 7E).

Discussion

Heart failure affects human health all over the world. Interventional cardiovascular therapy is widely used to improve the clinical outcomes of patients with heart failure (Esposito et al. 2018; Peng and Abdel-Latif 2019). Recovery of blood flow is necessary for rescuing ischemic myocardium. Nevertheless, myocardial revascularization may induce cardiomyocyte injury (Xiao et al. 2018). To imitate ischemic cell injury *in vivo*, we established cell model by usage of oxygen glucose deprivation/reoxygenation. In our study, as expected, the treatment of oxygen glucose deprivation/reoxygenation significantly decreased cell viability and promoted cell apoptosis and level of collagens.

Emerging studies showed that lncRNA played a role in physiological or pathological processes (Jathar et al. 2017; Peng et al. 2017). In ischemic heart failure, lncRNA PFL facilitated cardiac fibrosis by competitively binding with let-7d (Liang et al. 2018). In addition, TTTY15 exacerbated hypoxia-induced cardiomyocyte injury through acting as a sponge of miR-455-5p (Huang et al. 2019). Previously, SOX2-OT was identified to be significantly upregulated in non-end-stage heart failure patients (Greco et al. 2016). In our study, the level of SOX2-OT was also promoted by oxygen glucose deprivation/reoxygenation treatment. Consistent with the previous study, knockdown of SOX2-OT improved cell viability and limited cell apoptosis and level of collagens, suggesting that cell injury was alleviated by SOX2-OT knock-down. Mechanistically, SOX2-OT was reported to function as a competitive endogenous RNA and to regulate mRNA levels by sponging miRNA in several tumors (Wo et al. 2019; Zhang and Li 2019). Hence, we hypothesized that SOX2-OT also acted in this pattern in H9c2 cells. After prediction and screening, miR-215-5p was confirmed to bind with SOX2-OT. Thereafter, we further explored the target gene of miR-215-5p with the assistance of bioinformatics analysis, ZEB2 was screened out and confirmed to be directly targeted by miR-215-5p. Moreover, miR-215-5p negatively regulated ZEB2 protein levels.

Zinc finger E-box binding homeobox 2 (ZEB2), a member of the Zfh1 family of 2-handed zinc finger/home-

odomain proteins, has been reported to promote the activation of cardiac fibroblast to accelerate cardiac fibrosis (Jahan et al. 2018). Additionally, ZEB2 also involved in collagen fibrogenesis in Mowat-Wilson syndrome and Ehlers-Danlos syndrome (Teraishi et al. 2017). In the current research, rescue assay delineated that ZEB2 overexpression reversed the effects of SOX2-OT on cell viability, apoptosis and the level of collagens.

For the first time, we explored the role of SOX2-OT in ischemic heart failure *in vivo* and *in vitro*. All experimental results showed that SOX2-OT aggravated H9c2 cell injury via the miR-215-5p/ZEB2 axis *in vitro* and promoted heart failure in a rat model, suggesting that SOX2-OT may serve as a potential target for ischemic heart failure improvement. However, there may be other molecular mechanisms of SOX2-OT in H9c2 cells, which deserves further exploration in the future.

Conflict of Interest

The authors declare no conflict of interest.

References

Boully, C. & Hanon, O. (2015) Heart failure and comorbidities. *Geriatr Psychol Neuropsychiatr Vieil*, **13** Suppl 1, 13-22.

Cai, Y., Yu, X., Hu, S. & Yu, J. (2009) A brief review on the mechanisms of miRNA regulation. *Genomics Proteomics Bioinformatics*, **7**, 147-154.

Chen, H., Wang, X., Yan, X., Cheng, X., He, X. & Zheng, W. (2018) LncRNA MALAT1 regulates sepsis-induced cardiac inflammation and dysfunction via interaction with miR-125b and p38 MAPK/NFkappaB. *Int. Immunopharmacol.*, **55**, 69-76.

Curran, J., Burkhoff, D. & Kloner, R.A. (2019) Beyond reperfusion: acute ventricular unloading and cardioprotection during myocardial infarction. *J. Cardiovasc. Transl. Res.*, **12**, 95-106.

ENCODE Project Consortium (2004) The ENCODE (ENCyclopedia Of DNA Elements) Project. *Science*, **306**, 636-640.

ENCODE Project Consortium (2012) An integrated encyclopedia of DNA elements in the human genome. *Nature*, **489**, 57-74.

Esposito, M.L., Zhang, Y., Qiao, X., Reyelt, L., Paruchuri, V., Schnitzler, G.R., Morine, K.J., Annamalai, S.K., Bogins, C., Natov, P.S., Pedicini, R., Breton, C., Mullin, A., Mackey, E.E., Patel, A., et al. (2018) Left ventricular unloading before reperfusion promotes functional recovery after acute myocardial infarction. *J. Am. Coll. Cardiol.*, **72**, 501-514.

Greco, S., Zaccagnini, G., Perfetti, A., Fuschi, P., Valaperta, R., Voellenkle, C., Castelvecchio, S., Gaetano, C., Finato, N., Beltrami, A.P., Menicanti, L. & Martelli, F. (2016) Long noncoding RNA dysregulation in ischemic heart failure. *J. Transl. Med.*, **14**, 183.

Gryshkova, V., Fleming, A., McGhan, P., De Ron, P., Fleurance, R., Valentin, J.P. & Nogueira da Costa, A. (2018) miR-21-5p as a potential biomarker of inflammatory infiltration in the heart upon acute drug-induced cardiac injury in rats. *Toxicol. Lett.*, **286**, 31-38.

Henry, T.D. & Armstrong, P.W. (2016) The choice is reperfusion therapy: but which one? *JACC Cardiovasc. Interv.*, **9**, 2021-2023.

Heusch, G. & Gersh, B.J. (2017) The pathophysiology of acute myocardial infarction and strategies of protection beyond reperfusion: a continual challenge. *Eur. Heart J.*, **38**, 774-784.

Huang, S., Tao, W., Guo, Z., Cao, J. & Huang, X. (2019) Suppression of long noncoding RNA TTTY15 attenuates hypoxia-induced cardiomyocytes injury by targeting miR-455-5p. *Gene*, **701**, 1-8.

Huang, Y. (2018) The novel regulatory role of lncRNA-miRNA-mRNA axis in cardiovascular diseases. *J. Cell. Mol. Med.*, **22**, 5768-5775.

Huynh, K. (2016) Heart failure: ketone bodies as fuel in heart failure. *Nat. Rev. Cardiol.*, **13**, 122-123.

Jahan, F., Landry, N.M., Rattan, S.G., Dixon, I.M.C. & Wigle, J.T. (2018) The functional role of zinc finger E box-binding homeobox 2 (Zeb2) in promoting cardiac fibroblast activation. *Int. J. Mol. Sci.*, **19,** 3207.

Jathar, S., Kumar, V., Srivastava, J. & Tripathi, V. (2017) Technological developments in lncRNA biology. *Adv. Exp. Med. Biol.*, **1008**, 283-323.

Liang, H., Pan, Z., Zhao, X., Liu, L., Sun, J., Su, X., Xu, C., Zhou, Y., Zhao, D., Xu, B., Li, X., Yang, B., Lu, Y. & Shan, H. (2018) LncRNA PFL contributes to cardiac fibrosis by acting as a competing endogenous RNA of let-7d. *Theranostics*, **8**, 1180-1194.

Lu, T.X. & Rothenberg, M.E. (2018) MicroRNA. *J. Allergy Clin. Immunol.*, **141**, 1202-1207.

Lu, W., Zhu, L., Ruan, Z.B., Wang, M.X., Ren, Y. & Li, W. (2018) HOTAIR promotes inflammatory response after acute myocardium infarction by upregulating RAGE. *Eur. Rev. Med. Pharmacol. Sci.*, **22**, 7423-7430.

Peng, H. & Abdel-Latif, A. (2019) Cellular therapy for ischemic heart disease: an update. *Adv. Exp. Med. Biol.*, **1201**, 195-213.

Peng, W.X., Koirala, P. & Mo, Y.Y. (2017) LncRNA-mediated regulation of cell signaling in cancer. *Oncogene*, **36**, 5661-5667.

Rossello, X., Hall, A.R., Bell, R.M. & Yellon, D.M. (2016) Characterization of the Langendorff perfused isolated mouse heart model of global ischemia-reperfusion injury: impact of ischemia and reperfusion length on infarct size and LDH release. *J. Cardiovasc. Pharmacol. Ther.*, **21**, 286-295.

Ruggeri, C., Gioffre, S., Chiesa, M., Buzzetti, M., Milano, G., Scopece, A., Castiglioni, L., Pontremoli, M., Sironi, L., Pompilio, G., Colombo, G.I. & D'Alessandra, Y. (2018) A specific circulating microRNA cluster is associated to late differential cardiac response to doxorubicin-induced cardiotoxicity in vivo. *Dis. Markers*, **2018**, 8395651.

Tai, Y., Ji, Y., Liu, F., Zang, Y., Xu, D., Ma, S., Qin, L. & Ma, J. (2019) Long noncoding RNA SOX2-OT facilitates laryngeal squamous cell carcinoma development by epigenetically inhibiting PTEN via methyltransferase EZH2. *IUBMB Life*, **71**, 1230-1239.

Tang, Y., Wang, Y., Park, K.M., Hu, Q., Teoh, J.P., Broskova, Z., Ranganathan, P., Jayakumar, C., Li, J., Su, H., Tang, Y., Ramesh, G. & Kim, I.M. (2015) MicroRNA-150 protects the mouse heart from ischaemic injury by regulating cell death. *Cardiovasc. Res.*, **106**, 387-397.

Teraishi, M., Takaishi, M., Nakajima, K., Ikeda, M., Higashi, Y., Shimoda, S., Asada, Y., Hijikata, A., Ohara, O., Hiraki, Y., Mizuno, S., Fukada, T., Furukawa, T., Wakamatsu, N. & Sano, S. (2017) Critical involvement of ZEB2 in collagen fibrillogenesis: the molecular similarity between Mowat-Wilson syndrome and Ehlers-Danlos syndrome. *Sci. Rep.*, **7**, 46565.

Uchida, S. & Dimmeler, S. (2015) Long noncoding RNAs in cardiovascular diseases. *Circ. Res.*, **116**, 737-750.

Wang, Z., Tan, M., Chen, G., Li, Z. & Lu, X. (2017) LncRNA SOX2-OT is a novel prognostic biomarker for osteosarcoma patients and regulates osteosarcoma cells proliferation and motility through modulating SOX2. *IUBMB Life*, **69**, 867-876.

Wei, C.X., Wong, H., Xu, F., Liu, Z., Ran, L. & Jiang, R.D. (2018) IRF4-induced upregulation of lncRNA SOX2-OT promotes cell proliferation and metastasis in cholangiocarcinoma by regulating SOX2 and PI3K/AKT signaling. *Eur. Rev. Med. Pharmacol. Sci.*, **22**, 8169-8178.

Wo, Q., Zhang, D., Hu, L., Lyu, J., Xiang, F., Zheng, W., Shou, J. & Qi, X. (2019) Long noncoding RNA SOX2-OT facilitates prostate cancer cell proliferation and migration via miR-369-3p/CFL2 axis. *Biochem. Biophys. Res. Commun.*, **520**, 586-593.

Xiao, J., Xu, F., Yang, C.L., Chen, W.Q., Chen, X., Zhang, H., Wei, Z.J. & Liu, J.P. (2018) Preferred revascularization strategies in patients with ischemic heart failure: a meta-analysis. *Curr. Med. Sci.*, **38**, 776-784.

Zhang, E. & Li, X. (2019) LncRNA SOX2-OT regulates proliferation and metastasis of nasopharyngeal carcinoma cells through miR-146b-5p/HNRNPA2B1 pathway. *J. Cell. Biochem.*, **120**, 16575-16588.

Zhang, R., Wang, J., Liu, B., Wang, W., Fan, X., Zheng, B., Yuan, Q., Xue, M., Xu, F., Guo, P. & Chen, Y. (2020) Differentially expressed lncRNAs, miRNAs and mRNAs with associated ceRNA networks in a mouse model of myocardial ischemia/reperfusion injury. *Mol. Med. Rep.*, **22**, 2487-2495.

Zhou, G., Li, C., Feng, J., Zhang, J. & Fang, Y. (2018) lncRNA UCA1 is a novel regulator in cardiomyocyte hypertrophy through targeting the miR-184/HOXA9 axis. *Cardiorenal Med.*, **8**, 130-139.

Zou, Y., Wang, Y., Rong, Z., Wei, B., Liu, Y., Song, Z., Li, W., Hu, E., Deng, G., He, Y., Lv, J., Chen, L. & Li, W. (2020) A susceptibility biomarker identification strategy based on significantly differentially expressed ceRNA triplets for ischemic cardiomyopathy. *Biosci. Rep.*, **40,** BSR20191731.